Rare Metal Materials and Engineering
Volume 54, Issue 2, February 2025
Available online at www.rmme.ac.cn

Science Press

Cite this article as: Wang Xuanli, Li Wei. Relationship Between Stress and Texture in $L1_0$-FePt Thin Films[J]. Rare Metal Materials and Engineering, 2025, 54(02): 337-342. https://doi. org/10.12442/j. issn. 1002-185X.20240594.

ARTICLE

Relationship Between Stress and Texture in $L1_0$-FePt Thin Films

Wang Xuanli[1], Li Wei[2]

[1] School of Materials Science and Engineering, Inner Mongolia University of Science & Technology, Baotou 014010, China; [2] Instrumental Analysis Center, Inner Mongolia University of Science & Technology, Baotou 014010, China

Abstract: Impact of texture type on the magnetic properties of ultrahigh density perpendicular magnetic recording media $L1_0$-FePt thin film was investigated, so were the texture formation and evolution mechanism. Reuss, Voigt, and Hill models were used to determine the anisotropic elastic modulus of $L1_0$-FePt thin film with fiber texture. Then, the elastic strain energies of thin films under various stress conditions were calculated. Results reveal that the stress condition has a significant influence on the fiber texture evolution. When the $L1_0$-FePt thin film is subjected to compressive in-plane strain prior to ordering phase transformation, the formation of {100} fiber texture is promoted. On the contrary, the ordering phase transformation under tensile in-plane strain promotes the {001} fiber texture formation.

Key words: $L1_0$-FePt film; texture; stress; elastic modulus

Recently, it is noticed that fiber textures in thin films are critical for the performance control of functional materials, particularly for $L1_0$-FePt thin film in perpendicular magnetic recording hard disks. Because <001> axis is the most easily magnetized axis when $L1_0$-FePt thin film has strong {001} texture, the thin film can exhibit excellent perpendicular magnetic anisotropy to meet the application requirements[1]. As a result, the research on fiber texture of $L1_0$-FePt thin film has attracted extensive attention. Many approaches have been proposed to produce $L1_0$-FePt thin films with strong {001} fiber texture, including alternating deposition of Fe and Pt, utilization of single crystal substrate, addition of seed layer[2–5], magnetic field annealing+quick annealing[6–7], and film thickness adjustment[8–10]. How to enhance the {001} fiber texture in $L1_0$-FePt thin films has been the focus in most researches, but the texture formation, evolution mechanism, and texture control are rarely studied.

In the thin films, the anisotropy of strain energy and surface energy is the primary factor inducing the preferred growth of grains and the formation of fiber texture[11–12]. The elastic strain energy within thin films is intricately interconnected with the stress-strain and it is susceptible to modulation by external factors. These influences primarily originate from the residual strain in as-deposited thin films, the thermal strain resulting from disparities in thermal expansion coefficients between the film and substrate materials, and the strain induced by volumetric contraction of thin films due to defect annihilation and grain growth[13]. In addition to the aforementioned strains, the strain caused by disorder-to-order phase transition exists in FePt thin films. As-deposited FePt thin film has disordered face-centered cubic (fcc) structure, which is subjected to ordering phase transformation after annealing, thus forming ordered $L1_0$ phase with tetragonal structure. During the ordering phase transformation, the structure of FePt thin film changes, which leads to change in lattice constant so as to generate transformation strain. The stress state of FePt film strongly affects the grain growth orientation and influences the formation of fiber texture.

Hence, the formation and evolution mechanisms of fiber texture in $L1_0$-FePt thin films were investigated in this research. The anisotropic strain energy in $L1_0$-FePt thin films was calculated, and the influence of the changes in external stress on their fiber textures was analyzed, providing an effective reference for the preparation of $L1_0$-FePt thin films

Received date: September 13, 2024
Foundation item: Inner Mongolia Natural Science Foundation Project (2020LH05028)
Corresponding author: Li Wei, Ph. D., Professor, Instrumental Analysis Center, Inner Mongolia University of Science & Technology, Baotou 014010, P. R. China, Tel: 0086-472-5288100, E-mail: liwei_imust@126.com

with strong {001} fiber textures.

1 Calculation

1.1 Anisotropic elastic modulus

Elastic modulus is anisotropic due to different interatomic binding forces along different crystal orientations[14]. The anisotropic strain energy in $L1_0$-FePt thin films could be accurately calculated through the elastic constant and elastic modulus of different crystal planes in the films.

Reuss, Voigt, and Hill models were employed to calculate the macro-elastic constant of polycrystals. Reuss model is a iso-stress model after averaging the elastic flexibility coefficients of all grains along different orientations. As for Voigt model (iso-strain model), the elastic rigidity coefficients of all grains along different orientations were averaged. The elastic constants calculated by these two models were the upper and lower limits of actual value. Hill model expresses the elastic constant of a material by taking the arithmetic mean of the results calculated by the abovementioned models[15]. Orientation distribution function (ODF) describes the three-dimensional spatial distribution of textures, and it is mainly applied to analyze the textures of various polycrystalline materials. The elastic constant of anisotropic materials deviates from that of isotropic materials to a great extent. Therefore, ODF could be used to calculate the elastic constant, denote the relationship between texture coefficient and elastic constant, quantitatively analyze the change in elastic constant with the texture, and further clarify the stress-texture relationship in FePt thin films. As shown in Fig. 1, the sample coordinate system P_i and crystal coordinate system K_i of polycrystalline film could be defined to describe the crystal orientations in polycrystals. As for the crystal coordinate system, three mutually perpendicular crystal orientations were chosen according to the crystal symmetry. Generally, the crystal coordinate system does not overlap with the sample coordinate system, and the included angle between specific axes could be expressed by Euler angles (φ_1, ϕ, φ_2).

During calculation, the elastic constant should to be transformed from the crystal coordinate system to the sample coordinate system via a transformation matrix, as follows:

$$C'_{ijkl} = a_{im}a_{jn}a_{ko}a_{lp}C_{mnop} \tag{1}$$

$$S'_{ijkl} = a_{im}a_{jn}a_{ko}a_{lp}S_{mnop} \tag{2}$$

where C'_{ijkl} and S'_{ijkl} represent the elastic rigidity coefficient and elastic flexibility coefficient in the sample coordinate system, respectively; C_{mnop} and S_{mnop} stand for the monocrystal elastic rigidity coefficient and monocrystal elastic flexibility coefficient in the crystal coordinate system, respectively; a represents transformation matrix from the sample coordinate system to the crystal coordinate system; subscripts i, j, k, l, m, n, o, and p represent different matrices. The transformation matrix could be expressed by Euler angles to facilitate the integration of Euler space in statistical calculation, as follows:

$$a_{ij} = \begin{bmatrix} \cos\varphi_1\cos\varphi_2 - \sin\varphi_1\sin\varphi_2\cos\phi & \sin\varphi_1\cos\varphi_2 + \cos\varphi_1\sin\varphi_2\cos\phi & \sin\varphi_2\sin\phi \\ -\cos\varphi_1\sin\varphi_2 - \sin\varphi_1\cos\varphi_2\cos\phi & -\sin\varphi_1\sin\varphi_2 + \cos\varphi_1\cos\varphi_2\cos\phi & \cos\varphi_2\sin\phi \\ \sin\varphi_1\sin\phi & -\cos\varphi_1\sin\phi & \cos\phi \end{bmatrix} \tag{3}$$

Since the $L1_0$-FePt thin film has a tetragonal structure with lattice constant $a=b\neq c$, the transformation matrix a_{ij} should be multiplied by coefficient matrix T:

$$T = \begin{bmatrix} 1 & 0 & 0 \\ 0 & 1 & 0 \\ 0 & 0 & c/a \end{bmatrix} \tag{4}$$

1.1.1 Reuss model

In Reuss model, the average macro-elastic flexibility coefficient S'_{ijkl} of polycrystal materials should be the probability-weighted average of monocrystal elastic flexibility coefficients (S_{mnop}) of all grains based on their spatial orientation distribution[16]. The macro-elastic constant could be solved through the average value of elastic constants of all grains in their testing orientations, as expressed by Eq. (5), as follows:

$$\begin{aligned} \overline{S}^{R}_{ijkl} &= \frac{1}{8\pi^2}\int_{\Omega}^{2\pi} S'_{ijkl}\cdot f(g)\,\mathrm{d}g \\ &= \frac{1}{8\pi^2}\int_0^{2\pi}\int_0^{\pi}\int_0^{2\pi} a_{im}a_{jn}a_{ko}a_{lp}S_{mnop}f(g)\sin\phi\,\mathrm{d}\phi\,\mathrm{d}\varphi_1\,\mathrm{d}\varphi_2 \end{aligned} \tag{5}$$

where $f(g)$ denotes the normalized ODF, g represents the orientation, and Ω represents the orientation space of grains. The rigidity coefficient in Reuss model could be obtained by finding the inverse matrix of flexibility matrix, as expressed by Eq.(6), as follows:

$$\overline{C}^{R}_{ijkl} = \left[\overline{S}^{R}_{ijkl}\right]^{-1} \tag{6}$$

If the material possesses an ideal fiber texture, the abovementioned equation could be simplified, as follows:

$$\left\langle \overline{S}^{R}_{ijkl} \right\rangle^{hkl} = \frac{1}{2\pi}\int_0^{2\pi} S'_{ijkl}f(g)\,\mathrm{d}\varphi_1 \tag{7}$$

1.1.2 Voigt model

Similar to Reuss model, the average macro-elastic rigidity coefficient could be obtained by solving the probability-

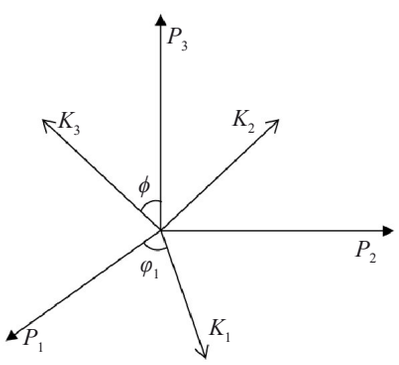

Fig.1 Schematic diagram of crystal and sample coordinate system of polycrystal

weighted average of monocrystal elastic rigidity coefficients of all grains in the crystal coordinate system according to their spatial orientation distribution. If the orientation correlations among adjacent grains, grain shape, and intergranular interaction were ignored, the elastic constant could be expressed by Eq.(8), as follows:

$$\overline{C}^{\mathrm{V}}_{\mathrm{ijkl}} = \frac{1}{8\pi^2}\int_{\Omega}^{2\pi} C'_{\mathrm{ijkl}} \cdot f(g)\,\mathrm{d}g = \frac{1}{8\pi^2}\int_0^{2\pi}\int_0^{\pi}\int_0^{2\pi} a_{\mathrm{im}}a_{\mathrm{jn}}a_{\mathrm{ko}}a_{\mathrm{lp}}C_{\mathrm{mnop}} f(g)\sin\phi\,\mathrm{d}\phi\,\mathrm{d}\varphi_1\,\mathrm{d}\varphi_2 \quad (8)$$

When the material possesses ideal fiber texture, one or two parameters among the three Euler angles (φ_1, ϕ, φ_2) can be fixed. In this case, Eq.(8) could be simplified into Eq.(9), as follows:

$$\left\langle \overline{C}^{\mathrm{V}}_{\mathrm{ijkl}} \right\rangle^{hkl} = \frac{1}{2\pi}\int_0^{2\pi} C'_{\mathrm{ijkl}} f(g)\,\mathrm{d}\varphi_1 \quad (9)$$

Then, the transformation matrix a_{ij} was substituted into Eq.(7) and Eq.(9) to solve the elastic flexibility coefficient and elastic rigidity coefficient of this material with ideal fiber texture under corresponding coordinate systems, respectively.

1.1.3 Hill model

Based on the results of Reuss and Voigt models, the arithmetic mean of macro-flexibility coefficient and rigidity coefficient of the material could be solved as Hill approximate value, as follows:

$$\begin{aligned} \overline{S}^{\mathrm{H}}_{\mathrm{ijkl}} &= \frac{1}{2}\left\{\overline{S}^{\mathrm{R}}_{\mathrm{ijkl}} + \left[\overline{C}^{\mathrm{V}}_{\mathrm{ijkl}}\right]^{-1}\right\} \\ \overline{C}^{\mathrm{H}}_{\mathrm{ijkl}} &= \frac{1}{2}\left\{\overline{C}^{\mathrm{R}}_{\mathrm{ijkl}} + \left[\overline{S}^{\mathrm{V}}_{\mathrm{ijkl}}\right]^{-1}\right\} \end{aligned} \quad (10)$$

The expression of Hooke's law is as follows:

$$\begin{aligned} \sigma_{\mathrm{ij}} &= C_{\mathrm{ijkl}}\varepsilon_{\mathrm{kl}} \\ \varepsilon_{\mathrm{ij}} &= S_{\mathrm{ijkl}}\sigma_{\mathrm{kl}} \end{aligned} \quad (11)$$

where C_{ijkl} is the elastic rigidity coefficient, presenting the relationship between two second-order tensors (stress σ and strain ε) generated under stress conditions; S_{ijkl} stands for the elastic flexibility coefficient. These two matrices were mutually reversible to some extent. Thus, $S_{\mathrm{ijkl}}=[C_{\mathrm{ijkl}}]^{-1}$ can be obtained.

After the subscripts of coefficients were simplified, the abovementioned Hooke's law could be expressed as $\sigma_q = C_{qr}\varepsilon_r$ and $\varepsilon_q = S_{qr}\sigma_r$ (q, r=1, 2, 3, 4, 5, 6), where the monocrystal elastic rigidity coefficient is assumed as C_{qr}, and the monocrystal elastic flexibility coefficient is assumed as S_{qr}. Then, C'_{qr} corresponding to any orientation (φ_1, ϕ, and φ_2) could be obtained through the transformational relation of tensors. Subsequently, the double-subscript matrix components of the rigidity coefficient were replaced by the four-subscript tensor components and then substituted into the coordination conversion formula of tensors, as follows:

$$C'_{qr} = C'_{\mathrm{ijkl}} = a_{\mathrm{im}}a_{\mathrm{jn}}a_{\mathrm{ko}}a_{\mathrm{lp}}C_{\mathrm{mnop}} \quad (12)$$

$$S'_{qr} = S'_{\mathrm{ijkl}} = a_{\mathrm{im}}a_{\mathrm{jn}}a_{\mathrm{ko}}a_{\mathrm{lp}}S_{\mathrm{mnop}} \quad (13)$$

The elastic constants of monocrystal $L1_0$-FePt materials are listed in Table 1[17]. On this basis, the elastic constants of isotropic $L1_0$-FePt materials under Reuss, Voigt, and Hill models could be solved, and the results are shown in Table 2.

When a fiber structure is generated in the $L1_0$-FePt thin film, the Miller index (h, k, l) of crystal face could be determined to express three Euler angles (φ_1, ϕ, φ_2), as follows:

$$\begin{aligned} \phi &= \arccos\frac{l}{\sqrt{h^2+k^2+l^2}} \\ \varphi_1 &= \arcsin\left(\frac{w}{\sqrt{u^2+v^2+w^2}}\cdot\sqrt{\frac{h^2+k^2+l^2}{h^2+k^2}}\right) \\ \varphi_2 &= \arccos\frac{k}{\sqrt{h^2+k^2}} \end{aligned} \quad (14)$$

If the $L1_0$-FePt thin film has the ideal fiber textures, its Miller index can be substituted into Eq. (7, 9 – 10), and the results are shown in Table 3.

When the thin film material is isotropic, its biaxial elastic modulus is correlated with Young's modulus and Poisson's ratio. The effect of anisotropy must be considered when fiber textures exist in the thin film, i. e., grains growing along a specific orientation or on a specific crystal face in grains are parallel to the surface of the thin film. Under the sample coordinate system, the biaxial elastic modulus M of the thin film could be expressed by Eq.(15)[18], as follows:

$$M = C_{11} + C_{12} - \frac{2C_{13}^2}{C_{33}} \quad (15)$$

According to Eq. (13), Eq. (15) could be transformed into Eq.(16), as follows:

$$M^{\mathrm{V}} = \left[C^{\mathrm{F}}_{11}\right] + \left[C^{\mathrm{F}}_{12}\right] - \frac{2\left[C^{\mathrm{F}}_{13}\right]^2}{\left[C^{\mathrm{F}}_{33}\right]} \quad (16)$$

$$\begin{aligned} \left[C^{\mathrm{F}}_{11}\right] + \left[C^{\mathrm{F}}_{12}\right] &= C_{11} + C_{12} - C_0^{\mathrm{T}}\Gamma^{\mathrm{T}}_{hkl} + 2Z\left(C_1^{\mathrm{T}}Z + 2\Delta C_{12} + 2\Delta C_{66}\right) + 2C_{16}Z_1 \\ \left[C^{\mathrm{F}}_{13}\right] &= C_{13} + C_0^{\mathrm{T}}\Gamma^{\mathrm{T}}_{hkl} + Z\left\{C_1^{\mathrm{T}}(1-2Z) - \Delta C_{12}\right\} - 2C_{16}Z_1 \\ \left[C^{\mathrm{F}}_{33}\right] &= C_{33} - 2C_0^{\mathrm{T}}\Gamma^{\mathrm{T}}_{hkl} - 4Z\left\{C_1^{\mathrm{T}}(1-Z) + \Delta C_{12} + 2\Delta C_{66}\right\} + 4C_{16}Z_1 \end{aligned} \quad (17)$$

$$C_0^{\mathrm{T}} = C_{11} - C_{12} - 2C_{66},\ C_1^{\mathrm{T}} = \Delta C_{11} - 2\Delta C_{12} - 4\Delta C_{66},\ \Delta C_{11} = C_{33} - C_{11},\ \Delta C_{12} = C_{13} - C_{12},\ \Delta C_{66} = C_{44} - C_{66}$$

$$Z = \frac{h^2+k^2}{2\left[h^2+k^2+(la/c)^2\right]^2},\ Z_1 = \frac{hk\left(h^2-k^2\right)}{\left[h^2+k^2+(la/c)^2\right]^2},\ \Gamma^{\mathrm{T}}_{hkl} = \frac{h^2k^2+\left(h^2+k^2\right)(la/c)^2}{\left[h^2+k^2+(la/c)^2\right]^2}$$

According to the abovementioned formula, the elastic

Table 1 Elastic constants of monocrystal $L1_0$-FePt thin film

C_{qr}/GPa						S_{qr}/MPa					
C_{11}	C_{12}	C_{13}	C_{33}	C_{44}	C_{66}	S_{11}	S_{12}	S_{13}	S_{33}	S_{44}	S_{66}
261	169	151	299	103	133	0.007 237	−0.003 630	−0.001 820	0.005 183	0.009 709	0.007 519

Table 2 Elastic constants of isotropic $L1_0$-FePt thin film (GPa)

Model	C_{11}	C_{12}	C_{13}	C_{33}	C_{44}	C_{66}
Voigt	249.0	169.0	161.0	226.0	65.0	68.0
Reuss	247.0	165.0	156.0	219.0	67.0	66.0
Hill	248.4	167.0	158.5	222.5	66.0	67.0

Table 3 Elastic constants of $L1_0$-FePt thin films with (*hkl*) fiber textures (GPa)

(*hkl*)	Model	C_{11}	C_{12}	C_{13}	C_{33}	C_{44}	C_{66}
(001)	Voigt	254.6	175.4	152.8	297.0	89.1	72.9
	Reuss	252.0	174.8	150.6	305.0	86.5	69.8
	Hill	253.3	175.1	151.7	298.0	87.8	71.5
(110)	Voigt	255.8	194.3	136.2	318.5	92.5	69.3
	Reuss	254.3	186.3	132.2	314.1	90.4	65.2
	Hill	255.5	190.6	134.2	316.3	91.5	67.3
(111)	Voigt	263.6	208.3	111.1	374.5	76.8	66.5
	Reuss	261.4	203.5	107.4	370.1	74.8	63.8
	Hill	262.5	205.9	109.5	372.3	75.8	65.3
(100)	Voigt	260.6	170.4	160.0	261.0	74.2	70.9
	Reuss	257.7	167.3	158.6	257.5	72.6	67.4
	Hill	259.2	168.6	159.3	259.3	73.3	69.2
(011)	Voigt	257.1	199.3	126.9	342.9	75.1	67.0
	Reuss	255.4	195.6	123.2	339.7	73.3	63.4
	Hill	256.3	197.5	124.6	341.3	74.2	65.2

modulus of $L1_0$-FePt thin film with ideal fiber texture can be obtained, and the results are shown in Table 4. It can be seen that $L1_0$-FePt thin film presents evidently different elastic properties under different textures, indicating that the elastic modulus of $L1_0$-FePt thin film is significantly impacted by the texture.

1.2 Elastic strain energy of $L1_0$-FePt thin films

$L1_0$-FePt thin film is impacted by external stress and transformation stress during growth, and the changes in stress state influence the strain energy in the thin film and finally lead to the formation of various fiber texture. Therefore, the strain energy of $L1_0$-FePt films under different stress states and the relationship between stress and texture are crucial to clarify the mechanisms of texture formation and evolution.

The thickness of $L1_0$-FePt thin film is much smaller than the substrate thickness, and the external stress is completely reflected by the binding force of the substrate against the thin film. Thus, the thin film is subjected to equivalent biaxial stress and the in-plane biaxial strain is generated. In this case, the in-plane strain of $L1_0$-FePt thin film is assumed to be a variable value from compressive strain to tensile strain, and the strain energy of $L1_0$-FePt thin film is discussed on this basis.

For polycrystalline films with fiber textures, the orientation of out-plane grains is consistent, but the in-plane grains show randomly distributed orientations. Under the in-plane equivalent biaxial stress, all in-plane grains generate the same strain. For simplification, all grains in the $L1_0$-FePt thin film are regarded as isometric crystals, and the in-plane strain can be denoted by the circumcircle radius of the crystal face, as shown in Fig. 2a. In addition, the [001] crystal orientation is designated as the *c* axis after ordering phase transformation. Fig. 2b shows the crystal coordinate system of $L1_0$-FePt thin film. In Fig. 2c, the grains along all orientations within the $L1_0$-FePt thin film before ordering phase transformation are considered as the circumcircle with radius *R* and those after ordering phase transformation are regarded as the circumcircle with radius R'. In this case, the strain generated by external stress and that by ordering phase transformation are effectively associated for accurate calculation of the strain

Table 4 Elastic properties of $L1_0$-FePt thin films with (*hkl*) fiber textures

Texture	Young's modulus, *E*/GPa	Biaxial elastic modulus, *M*/GPa	Poisson's ratio, *v*
(001)	241.43	277.48	0.355
(110)	253.87	333.17	0.373
(111)	216.83	406.05	0.411
(100)	201.48	234.83	0.357
(011)	210.89	362.23	0.403

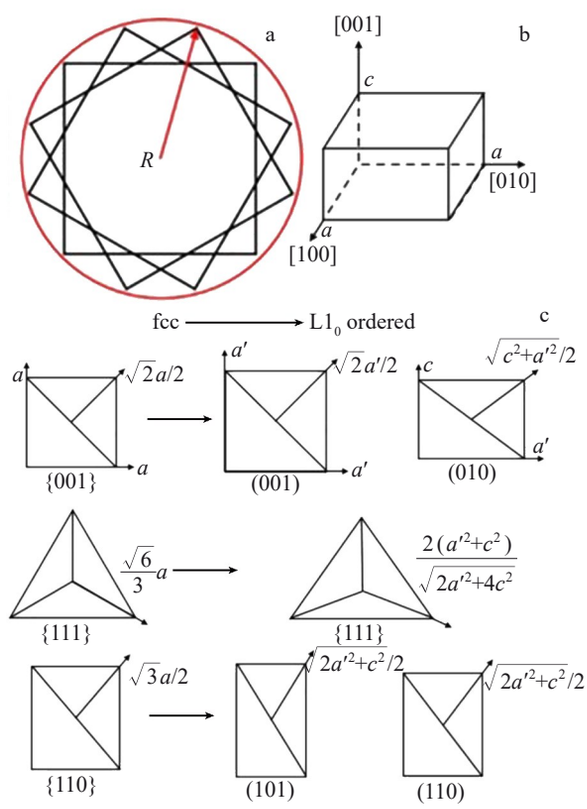

Fig.2 Schematic diagrams of in-plane strains of thin film: (a) unit volume circle; (b) crystal coordinate system of $L1_0$-FePt thin film; (c) change in radius of unit volume circle before and after ordering phase transformation of crystal faces along different orientations

energy of the $L1_0$-FePt thin film.

The strain energies of the $L1_0$-FePt thin film under ideal textures of {001}, {010}, {111}, {101}, and {110} are calculated. According to Fig.2c, in the case of ordering phase transformation, different transformation strains (ε_t) are generated on the crystal faces of different orientations, which can be expressed by the radius difference between the unit volume circle before and after ordering phase transformation, as follows:

$$\varepsilon_t = \frac{R' - R}{R} \tag{18}$$

The in-plane strain generated by external stress in the thin film before ordering phase transformation can be denoted by the coefficient k. The range of in-plane strain generated by the external environment to the $L1_0$-FePt thin film is assumed to be (− 0.03, 0.03), and the thin film suffers ordering phase transformation under different external stresses. Therefore, the elastic strain energy of $L1_0$-FePt thin films with different fiber textures can be denoted by Eq.(19), as follows:

$$W_{hkl} = M_{hkl}\left[\frac{R' - R(1+k)}{R(1+k)}\right]^2 \tag{19}$$

2 Results and Discussion

According to the anisotropic elastic modulus of $L1_0$-FePt thin film, the elastic strain energy of $L1_0$-FePt film under the combined action of external stress and phase change stress is obtained. The results are shown in Fig. 3. The calculation results show that the strain energies of $L1_0$-FePt thin films with different fiber textures are substantially influenced by the in-plane strain state.

When the ordering phase transformation occurs in the $L1_0$-FePt thin film, the in-plane compressive strain of 0 – 0.005 exists, the types of fiber textures vary less obviously based on the elastic strain energy, and the surface energy of the thin film is the main driving force for texture formation. When the in-plane compressive strain further increases from 0.005, the difference between fiber textures becomes obvious, the {100} plane in the thin film possesses the minimum strain energy, and the {001} plane has the maximum strain energy. With the further increase in the in-plane compressive strain, an increasingly evident difference of strain energy can be observed between {100} and {001} planes. The formation of {100} fiber textures in the $L1_0$-FePt thin film is facilitated by minimizing the strain energy when the thin film is subjected to ordering phase transformation under a large in-plane compressive strain. However, when it is at the in-plane tensile strain state, the {001} crystal face possesses the minimum strain energy. The difference of this crystal face from other crystal faces is more obvious with the increase in the in-plane tensile strain, thus promoting the formation of {001} fiber textures in the $L1_0$-FePt thin film.

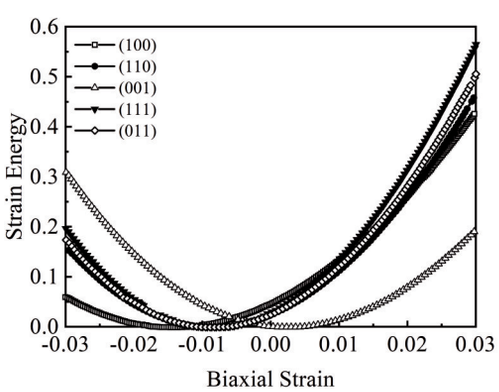

Fig.3 Strain energy in $L1_0$-FePt thin films under different in-plane biaxial strains

Hence, in order to obtain strong {001} fiber textures, $L1_0$-FePt thin films should be adjusted to reach the in-plane tensile stress state before the ordering phase transformation. Moreover, the larger the in-plane tensile strain, the better the formation of {001} fiber texture.

3 Conclusions

1) When $L1_0$-FePt thin film is at in-plane compressive stress state during ordering phase transformation, the formation of {100} fiber textures is promoted.

2) {001} fiber textures tend to appear when $L1_0$-FePt thin film is at tensile stress state.

3) The larger the in-plane tensile strain, the better the formation of {001} fiber texture, and the stronger the intensity of {001} fiber texture.

References

1 Zhang L, Takahashi Y K, Perumal A *et al*. *Journal of Magnetism and Magnetic Materials*[J], 2010, 322(18): 2658

2 Kang K, Zhang Z G, Papusoi C *et al*. *Applied Physics Letters*[J], 2004, 84(3): 404

3 Weisheit M. *Journal of Applied Physics*[J], 2004, 95(11): 7489

4 Hotta A, Ono T, Hatayama M *et al*. *Journal of Applied Physics*[J], 2014, 115(17): 17B712

5 Shima T, Moriguchi T, Mitani S *et al*. *Applied Physics Letters*[J], 2002, 80(2): 288

6 Liu L W, Hua L, Wei S *et al*. *Applied Surface Science*[J], 2012, 258(15): 5770

7 Ishio S, Narisawa T, Takahashi S *et al*. *Journal of Magnetism and Magnetic Materials*[J], 2012, 324(3): 295

8 Dang H G, Liu L W, Hao L *et al*. *Journal of Applied Physics*[J], 2014, 115(17): 17B711

9 Mei J K, Yuan F T, Liao W M *et al*. *IEEE Transactions on Magnetics*[J], 2011, 47(10): 3633

10 Sun A C, Hsu J H, Kuo P C *et al*. *Journal of Magnetism and Magnetic Materials*[J], 2007, 310(2): 2650

11 Thompson C V, Carel R. *Materials Science & Engineering B*[J], 1995, 32(3): 211

12 Ellis E A, Chmielus M, Lin M T *et al*. *Acta Materialia*[J], 2016, 61(19): 7121

13 Zeiger W, Brückner W, Schumann J *et al*. *Thin Solid Films*[J], 2000, 370(1–2): 315

14 Welzel U, Fréour S, Mittemeijer E J. *Philosophical Magazine*[J], 2005, 85(21): 2391
15 Noyan I C, Cohen J B. *Residual Stress: Measurement by Diffraction and Interpretation*[M]. Berlin: Springer, 1987
16 Bunge H J. *Materials Science Forum*[J], 1998, 273–275: 3
17 Müller M, Erhart P, Albe K. *Physical Review B*[J], 2007, 76(15): 155412
18 Feng H, Weaver M L. *Journal of Applied Physics*[J], 2006, 100(9): 093523
19 Mei J K, Yuan F T, Liao W M *et al*. *Journal of Applied Physics*[J], 2011, 109(7): 07A737

$L1_0$-FePt薄膜应力与织构的关系

王炫力[1]，李　玮[2]
(1. 内蒙古科技大学 材料科学与工程学院，内蒙古 包头 014010)
(2. 内蒙古科技大学 分析测试中心，内蒙古 包头 014010)

摘　要：探讨了织构的类型对超高密度垂直磁记录介质材料$L1_0$-FePt薄膜磁性能的影响及织构的形成和演化机制。通过Reuss、Voigt和Hill模型确定了具有纤维织构的$L1_0$-FePt薄膜的各向异性弹性模量，然后计算了薄膜在不同应力条件下的弹性应变能。结果表明，应力条件对纤维织构演变具有显著影响。$L1_0$-FePt薄膜在有序转变之前受到平面压缩应力能够促进{100}纤维织构的形成，而平面拉伸应变下的有序转变促进了{001}纤维织构的形成。

关键词：$L1_0$-FePt薄膜；织构；应力；弹性模量

作者简介：王炫力，女，1989年生，博士，讲师，内蒙古科技大学材料科学与工程学院，内蒙古 包头 014010，电话：0472-5288100，E-mail：wangxuanli917@163.com